# Pulse Shortening in Recirculating Planar Magnetrons

Nicholas M. Jordan, *Member, IEEE*, Geoffrey B. Greening, *Member, IEEE*, Steven C. Exelby, *Student Member, IEEE*, Drew A. Packard, *Student Member, IEEE*, Yue Ying Lau, *Fellow, IEEE*, and Ronald M. Gilgenbach, *Life Fellow, IEEE*

***Abstract*— Recirculating planar magnetron (RPM) experiments at the University of Michigan have utilized a 12-frame ultrafast intensified CCD camera to analyze the effect of plasma formation on microwave pulse duration. The RPM was driven by a -300-kV voltage pulse for 0.3–1.0 $\mu$s, with a 0.08–0.27-T axial magnetic field. The RPM has previously demonstrated peak microwave powers of over 150 MW, with typical microwave pulse durations of 50–150 ns, far shorter than the available voltage pulse. To investigate possible causes of pulse shortening, the RPM was imaged with both S-band (2 GHz) and L-band (1 GHz) anodes, as well as two different cathodes with substantially different anode–cathode (AK) gap widths and end caps. It was found that a smaller AK gap produced brighter plasma and allowed for improvements in temporal resolution of the imaging configuration at the expense of larger end-loss current. Many shots demonstrated a direct correlation between inter-vane anode plasma formation and a sharp reduction in RF power. Anode vane plasma is formed at the axial ends of the anode, indicating field enhancement effects. Contact resistance plasma was also observed at the back of anode vane cavities. Details of plasma formation are illustrated and methods for remediating these plasmas are proposed.**

***Index Terms*— Coherent radiation, electron beams, framing camera, high-power microwaves (HPMs), magnetrons, plasma, pulse shortening.**

## I. Introduction

PULSE-SHORTENING affects nearly all high-power microwave (HPM) devices, and the recirculating planar magnetron (RPM) [1], [2] is no exception. The exact mechanism responsible for microwave cessation in HPM devices varies, but common explanations and theories include cathode plasma expansion [3], anode plasma formation [4], multipactor RF window breakdown [5], poor RF contact [6], and generator impedance mismatch [7].

Pulse shortening in relativistic magnetron experiments, including those at the University of Michigan [8], is typically attributed to cathode plasma expansion [9]. These cylindrical relativistic magnetron experiments, however, produced microwave pulses of hundreds of nanoseconds in duration. Recent recirculating planar magnetron (RPM) experiments [10], [11] have exhibited short (50–150 ns), intense (150 MW) microwave bursts. Given the 2–3-cm anode–cathode (AK) gap present in the RPM, and typical gap closure rates of 1–4 cm/$\mu$s [12]–[14], the effective AK gap of the RPM does not change fast enough to explain the rapid pulse shortening that is observed. To determine other possible contributing factors, a series of imaging experiments was conducted.

Manuscript received November 2, 2017; revised December 18, 2017 and February 5, 2018; accepted February 8, 2018. Date of publication March 6, 2018; date of current version May 21, 2018. This work was supported in part by the Air Force Office of Scientific Research under Award FA9550-15-1-0097 and Award FA9550-15-1-0419, in part by ONR under Grant N00014-16-1-2353, in part by DEPS, and in part by L-3 Communications Electron Devices. The review of this paper was arranged by Editor J. Jelonnek. *(Corresponding author: Nicholas M. Jordan.)*

N. M. Jordan, S. C. Exelby, D. A. Packard, Y. Y. Lau, and R. M. Gilgenbach are with the Department of Nuclear Engineering and Radiological Sciences, University of Michigan, Ann Arbor, MI 48109 USA (e-mail: jordann@umich.edu; scxelb@umich.edu; drupac@umich.edu; yylau@umich.edu; rongilg@umich.edu).

G. B. Greening was with the Department of Nuclear Engineering and Radiological Sciences, University of Michigan, Ann Arbor, MI 48109 USA. He is now with the Beverly Microwave Division, Communications and Power Industries, Beverly, MA 01915 USA (e-mail: geoffrey.greening@cpii.com).

Color versions of one or more of the figures in this paper are available online at http://ieeexplore.ieee.org.

Digital Object Identifier 10.1109/TED.2018.2807739

## II. Experimental Configuration

The pulse shortening measurements were conducted using variants of the multifrequency recirculating planar magnetron (MFRPM) [15], driven by the Michigan Electron Long Beam Accelerator with a ceramic insulator stack (MELBA-C) [16]. MELBA-C provides a flat-top voltage pulse between −250 and −300 kV with a 120–150-ns rise time and adjustable pulse duration of 200–600 ns. A pair of pulsed electromagnets in a pseudo-Helmholtz configuration creates a nearly uniform axial magnetic field pointing toward the viewport, which was varied on a per-shot basis from 0.08 to 0.27 T. The magnetron was operated at base vacuum pressures of approximately $3 \times 10^{-4}$ Pa.

To accommodate existing hardware, the MFRPM was designed with axial extraction [17]. To gain access to an imaging port, one of the microwave extractors was removed and replaced by a copper-screened Lexan window, as shown in Fig. 1. While this necessarily meant that a calibrated power measurement could not be made during imaging tests, microwave signals were sampled with an uncalibrated B-dot antenna within the vacuum chamber, near the viewport. This probe could only provide relative amplitudes of the RF pulses, but provided precise temporal information, allowing microwave behavior to be correlated with observed plasma formation. The B-dot was sampled by a 6-GHz, 20 GSample/s

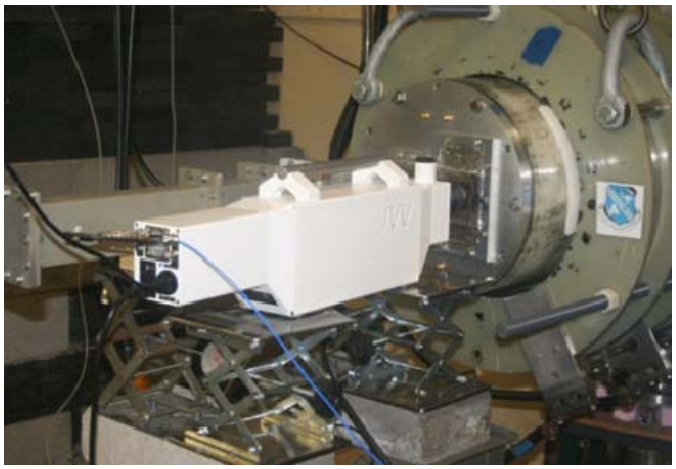

Fig. 1. UHSi-12 framing camera with an axial view of magnetron operation via a short focal distance lens. The microwave extractor is replaced by a copper-screened Lexan viewport. For scale, the vacuum chamber has a diameter of 45.7 cm.

Agilent 54855A oscilloscope. The high sampling rate of this oscilloscope allows direct collection of the 1- and 2-GHz microwave signals, and enables mode identification through time-frequency analysis.

In addition to this microwave diagnostic, the performance of the pulsed power system was monitored using a $CuSO_4$ resistive voltage divider for the cathode voltage, a pair of digitally integrated Rogowski coils for the magnetron entrance current, and a Pearson current transformer for the electromagnet current. Electromagnet current is subsequently correlated with an axial magnetic field value using Hall probe calibrations.

Initial magnetron imaging was accomplished with a modified Canon Rebel Xsi SLR camera (no IR filter), with an F5.6 aperture and a 400 ISO speed, placed directly in front of the copper-screened viewport. After capturing time-integrated images and ensuring a safe electromagnetic environment, the Canon SLR was replaced with the Invisible Vision UHSi-12 framing camera and Nikon DX AF-S Nikkor 18–55-mm lens, as shown in Fig. 1. The UHSi-12 can capture 12 frames at 200 million frames per second (5 ns per frame), has an image intensifier with up to 5000× gain, and has a spectral response of 450–850 nm. The approximate line of sight (and field of view) for these cameras is shown in Fig. 2(b).

All images focused on only the central 3–5 vanes of the anode structure. Simulations have indicated that electric field stresses are highest in this region [15], and wider field-of-view images taken during this experiment confirmed that the depth of plasma generation in the cavities exhibited a half-sine distribution peaked at the center vane.

The data were collected in three sets: the *L*-band (1 GHz) anode with the mode control cathode (MCC-1), the *S*-band (2 GHz) anode with the MCC-2, and the *L*-band anode with the MCC-2. In all configurations, a planar drift region was placed on the opposite side of the magnetron, as shown in Fig. 2(a).

The MCC is a slotted cathode designed to synchronize operation on each half of the RPM and decrease mode competition. Design details of the MCC can be found in [18]. MCC-1 is

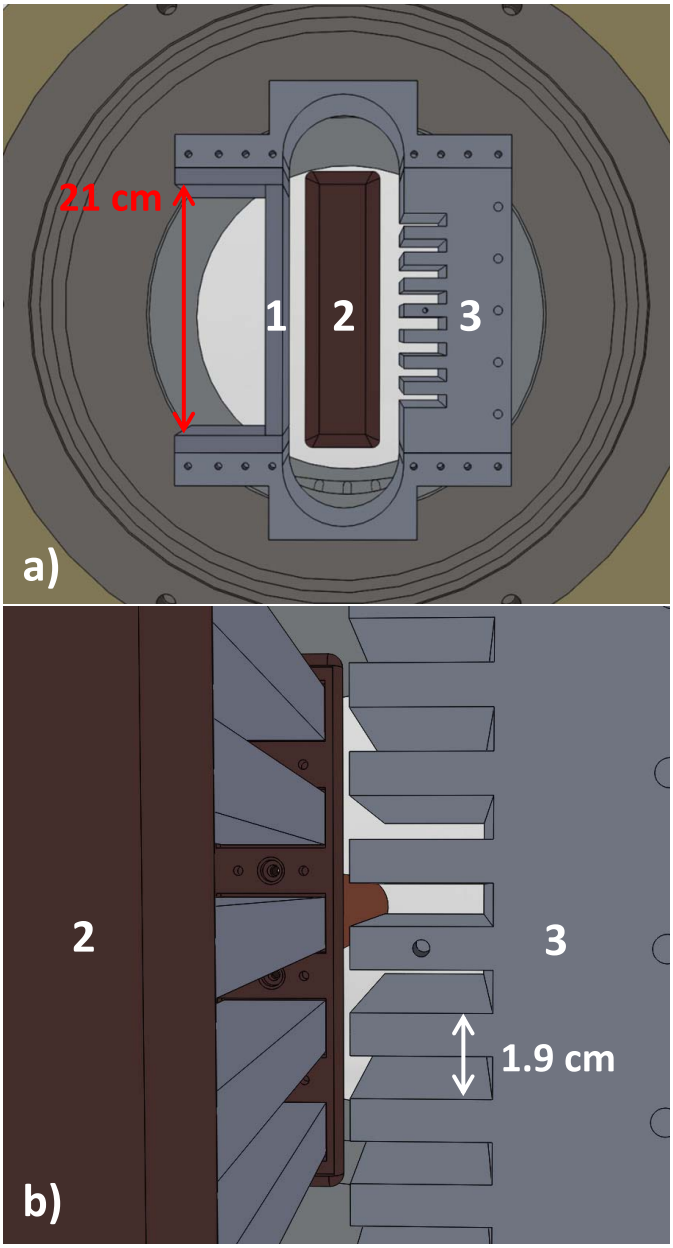


Fig. 2. (a) Axial view of the test chamber with a (1) planar drift region, (2) MCC-2 cathode, and (3) *S*-band anode. (b) Line of sight of the camera during imaging.

slightly narrower and results in an AK gap of 3.4 cm, compared to 2.6 cm for MCC-2. MCC-1 also has a larger end cap, greatly suppressing axial electron beam losses [19], [20]. This was a desirable feature, given the location of the cameras. Unfortunately, the larger AK gap reduces field intensity (and plasma self-emission), resulting in minimal light emission and requiring longer camera exposures. MCC-2 provided brighter plasma, allowing for camera exposures of 25–50 ns per frame.

## III. Experimental Results

### A. MCC-1 With L-Band Anode

Time-integrated SLR camera images provided clear evidence of substantial plasma formation during the course of an RPM shot. As shown in Fig. 3, in addition to the expected

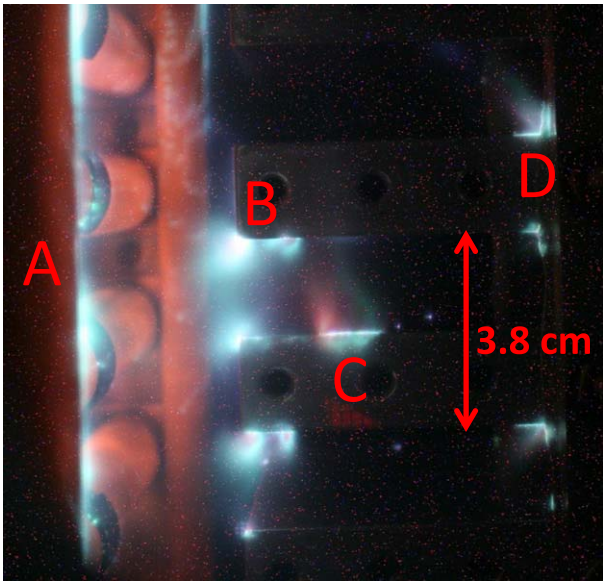


Fig. 3. Time-integrated SLR camera image of *L*-band oscillator with an MCC-1 cathode. Plasma formation is visible at the cathode (A), anode vane tips (B), between the anode vanes (C), and at metal contact surfaces (D).

cathode (A) and anode (B) plasma in the AK gap, there was consistent evidence of plasma formation between the anode vanes (C) and at the back of the anode (D).

The back of the anode (D) serves as the contact point for the ground path of the anode. Consequently, approximately a kiloampere of anode current flows through this location, and these images indicate the RF gasket material used is insufficient, resulting in poor electrical contact. As shown by time-resolved imaging, this plasma is formed during the microwave pulse and could adversely affect magnetron operation.

The long voltage and current pulse ($\sim$1 $\mu$s), relative to the microwave pulse duration ($\sim$100 ns), left considerable uncertainty as to when the plasma formed. To establish a narrower window for plasma formation, the framing camera was fielded to capture image sequences like those shown in Fig. 4. To collect sufficient light, the camera frame duration needed to be 150 ns. In this figure, outlines of the cathode and anode have been sketched in orange and white, respectively. As shown in Fig. 2(b), the available imaging port is positioned over the anode (rather than over the AK gap) and is angled slightly, so there is a parallax effect which makes the cathode plasma appear closer to the anode than it really is. To provide a reference in Fig. 4, the axial front and back of the cathode are denoted with orange lines. The images have also been recolored to improve contrast and filtered to minimize noise. Fig. 4(b), corresponding to peak microwave emission, still contains substantial noise even after filtering. These small, randomly distributed hotspots are not plasma, and are present on the images where the lens is completely covered, and on shots in which the camera is lead shielded. They are most intense during the microwave pulse and are likely the result of electromagnetic interference. The images in Fig. 4 were taken on the *L*-band anode, with the MCC-1 cathode, so the intervane spacing (1.9 cm) and the AK gap (3.4 cm) are both relatively large, and the resulting plasma was weak.

These images were taken on shot 14834, whose voltage, current, microwave emission, and camera timing are outlined in Fig. 5. The magnetic field for this shot was 0.13 T. Fig 4(a) occurs before microwave generation and shows no evidence of plasma formation. In Fig. 4(b), plasma forms at the cathode/anode surfaces, between the anode vanes and in the rear of the cavities, consistent with the time-integrated image in Fig. 3. This frame contains the entirety of the microwave pulse. These plasma hotspots grow in intensity in Fig. 4(c), before nearly extinguishing in Fig. 4(d). In Fig. 4(e)(well after peak power, current, and voltage), plasma reforms along the anode and cathode surfaces, growing again in intensity until Fig. 4(f), before extinguishing again after frame 12 (not shown).

This late-time plasma formation consistently corresponds to voltage and current reversal on the pulse power generator and is generally substantially brighter than early-time plasma. On shots with no current reversal, no late-time plasma is observed. Consequently, time-integrated images which appear to show severe plasma formation in the AK gap may be misleading, as the bulk of the emission occurs well after the microwave pulse has ceased.

### B. MCC-2 With S-Band Anode

A subsequent dataset captured plasma formation on the *S*-band anode and the MCC-2. This configuration had only a 2.6-cm AK gap, and produced much brighter plasma that allowed for frame durations as low as 25 ns. A sample set of frames from this dataset are shown in Fig. 6, where the surface of the *S*-band anode and the axial boundaries of the cathode have been sketched in yellow and black, respectively. The anode plasma predominantly formed on the axial edges of the anode vane closest to the camera. Consequently, the anode vanes have also been drawn slightly narrower than reality, so that they do not obscure the plasma hotspots.

In these time-resolved images, we again see evidence of intervane plasma formation in Fig. 6(b) which corresponds to a drop in microwave intensity. This spot (highlighted with a red dashed oval) is barely distinguishable from the background noise in this frame, but clearly continues to develop its intensity in subsequent frames. The location, persistence, growth, and repeatability (it appears here in many different shots) provide evidence that this is not simply noise. The magnetron briefly restarts in Fig. 6(c) and is again extinguished, with intense plasma formation in multiple cavities. Time-frequency analysis of this shot [21] indicates the magnetron shifts to a new operating frequency as the plasma forms. What appears to be a large, diffuse cathode plasma is actually light produced by the electron beam striking the Lexan window. As noted earlier, a disadvantage of the MCC-2 is its relatively small end caps, which do not confine the beam axially.

### C. MCC-2 With L-Band Anode

To analyze the effects of anode geometry, the *S*-band anode was replaced by the *L*-band anode for the final dataset. Given the larger feature sizes of this anode, the observed plasma was less intense and the minimum usable frame width was

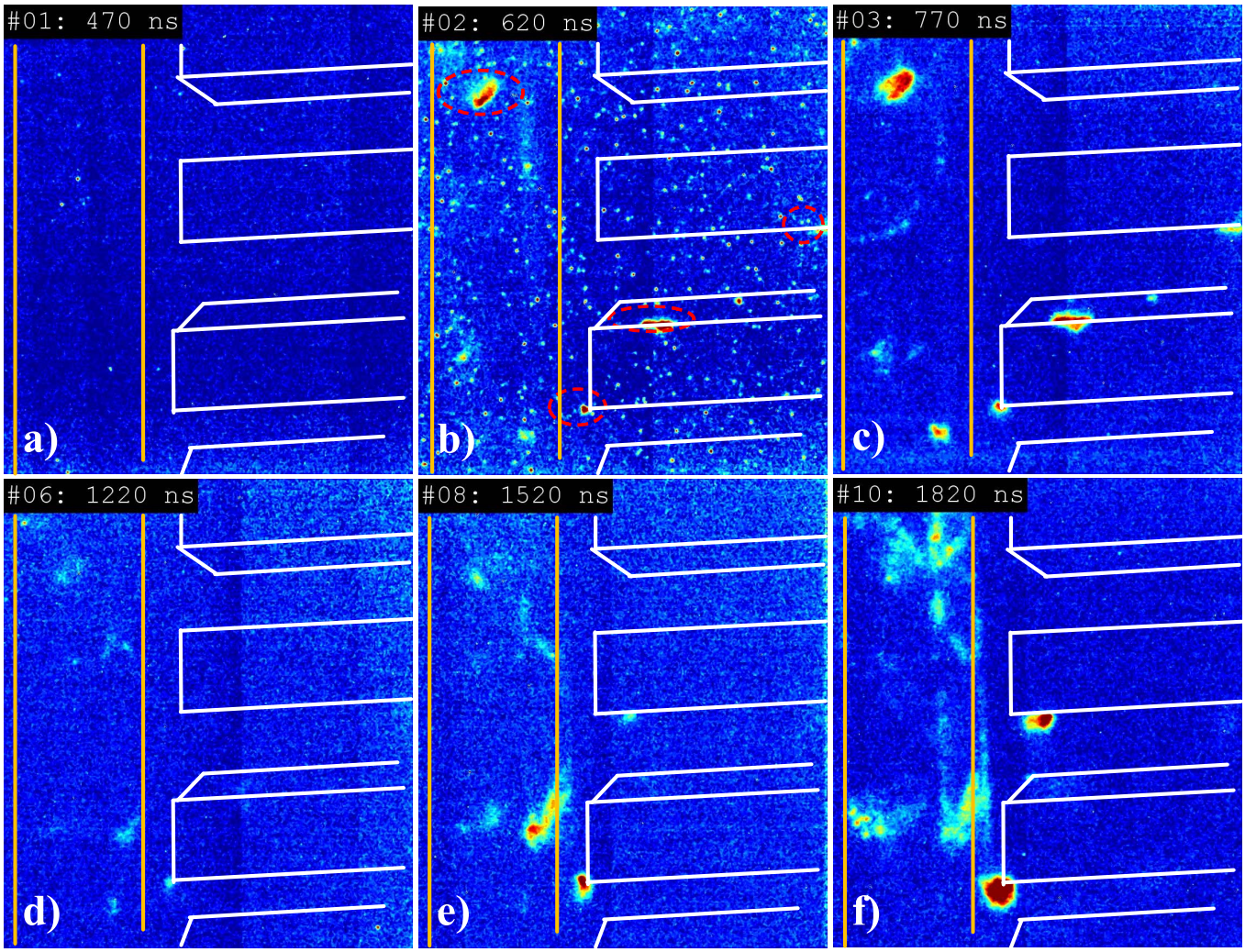


Fig. 4. Selected framing camera images from shot 14 834. Plasma forms during the microwave pulse, extinguishes, restarts as the pulse power driver current reverses, and then reaches peak intensity well after peak voltage/current.

50 ns. Again, there was intervane plasma generation which correlated with a sharp drop in microwave intensity, as shown in Fig. 7(b). The intervane plasma appears to be a small distance away from the anode surface. This is a result of the position of the camera [see Fig 2(b)]. This plasma is actually forming on the axial rear edge of the anode, closest to the pulsed power driver. The images in Figs. 4 and 6 exhibited plasma formation on the front axial edge of the anode, closest to the camera.

The intense plasma on the left side of Fig. 7(c) outlines the surface of the cathode, with central squares of low plasma intensity. These squares are the carbon velvet emission areas, while the rest of the cathode consists of aluminum coated with Glyptal insulating enamel. The Glyptal appears to be a strong source of plasma, likely due to electron back-bombardment and secondary emission. Alternative materials should be investigated to suppress emission from undesired regions of the cathode.

## IV. Discussion

There are a few noteworthy limitations of these experiments. First, removal of the microwave extractor results in a magnetron with an unloaded $Q$ of $\sim$1740 [11] and is not directly representative of typical operating conditions. The standard load of the MFRPM produced a loaded $Q$ of $\sim$150, while the tapered waveguide load resulted in a loaded $Q$ of $\sim$2200 [15]. Without microwave extraction, the electric fields present on the anode may be artificially high. However, MAGIC [22] particle-in-cell simulations of MFRPM operation indicated electric field strengths of over 200 kV/cm within the anode cavities, as shown in Fig. 8. These intense electric fields, coupled with electron impacts on the anode, could provide sufficient energy to liberate surface contaminants ($>$50 J/g [14]), creating an environment where intervane plasma formation could disrupt device operation. The observed plasma corresponds to regions of field enhancement and high RF fields, and likely has localized energy deposition that far exceeds the bulk energy density of the electron–anode interactions. Pulse shortening via RF-induced anode vane plasma has been postulated as a source of pulse shortening in other HPM devices [23] and in magnetrons at GW power levels [24].

Another limitation is the emissivity of the plasma. Previous work at Technion has demonstrated that plasma within a relativistic magnetron can be successfully imaged

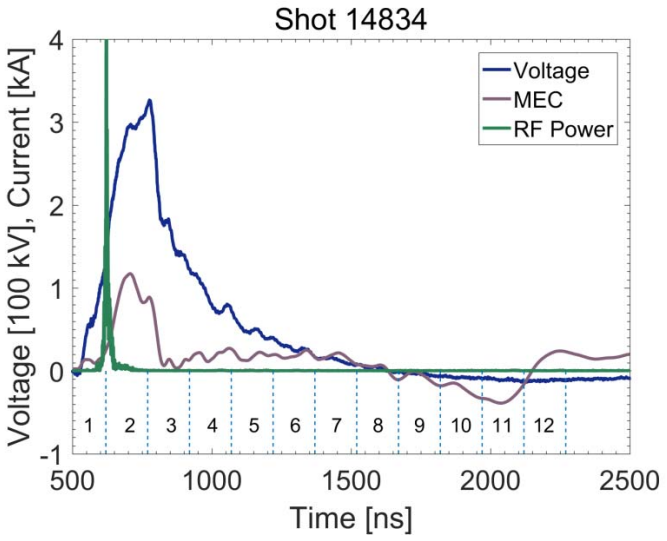


Fig. 5. Typical microwave pulse shortening in the RPM and MFRPM. Despite a voltage and current pulse lasting for several hundred nanoseconds, the microwave signal is only ~50 ns. MEC is a Rogowski coil measurement of magnetron entrance current. The RF power is uncalibrated and is given in arbitrary units. Camera frame widths are denoted by blue dashed lines. Late-time current reversal generates significant plasma within the device.

only where the plasma is relatively dense ($\sim 10^{14}/\text{cm}^3$) and warm (~5 eV) [25], [26]. If cold or low-density plasma exists within the device, it will not radiate enough to be visible on the framing camera. Cold plasma, however, is likely not contributing greatly to a reduction in device performance. If the plasma is absorbing energy that otherwise would be converted to microwaves, it will rapidly increase in temperature.

As initially postulated, the framing camera images do not indicate significant plasma expansion across the AK gap. To successfully cross the magnetic field lines and expand into the gap, this highly ionized plasma would need to be collisional and should rapidly heat up as it becomes the effective cathode surface. Previous imaging of relativistic magnetrons has been able to detect this expanding plasma with visible light diagnostics [12], [25]. In some images presented in this paper, such as in Fig. 7, it appears there is a low intensity of plasma filling the AK gap. In reality, it primarily forms along the surface of the cathode and its end caps. The previously mentioned parallax effect from the camera position creates the illusion the plasma has expanded into the AK gap, but true cathode plasma expansion would actually appear further to the right, past the outline of the anode vane tips.

While significant expansion was not observed, cathode plasma formation was evident, particularly for the *L*-band anode and MCC-2. It is likely that this plasma caused a small change in effective cathode radius and slightly detuned the beam synchronism condition. However, magnetic field parameter sweeps of the MFRPM indicate a fairly wide range of operating conditions [15], so a small change in effective radius should not be enough to explain the rapid decrease in microwave production.

Surface conditions have been identified as a major contributor to pulse shortening in HPM devices [9]. The data presented here were collected in sets of 15–60 shots, with the vacuum chamber only opened to atmosphere between sets. No long-term conditioning trends were observed, but the first ~3 shots

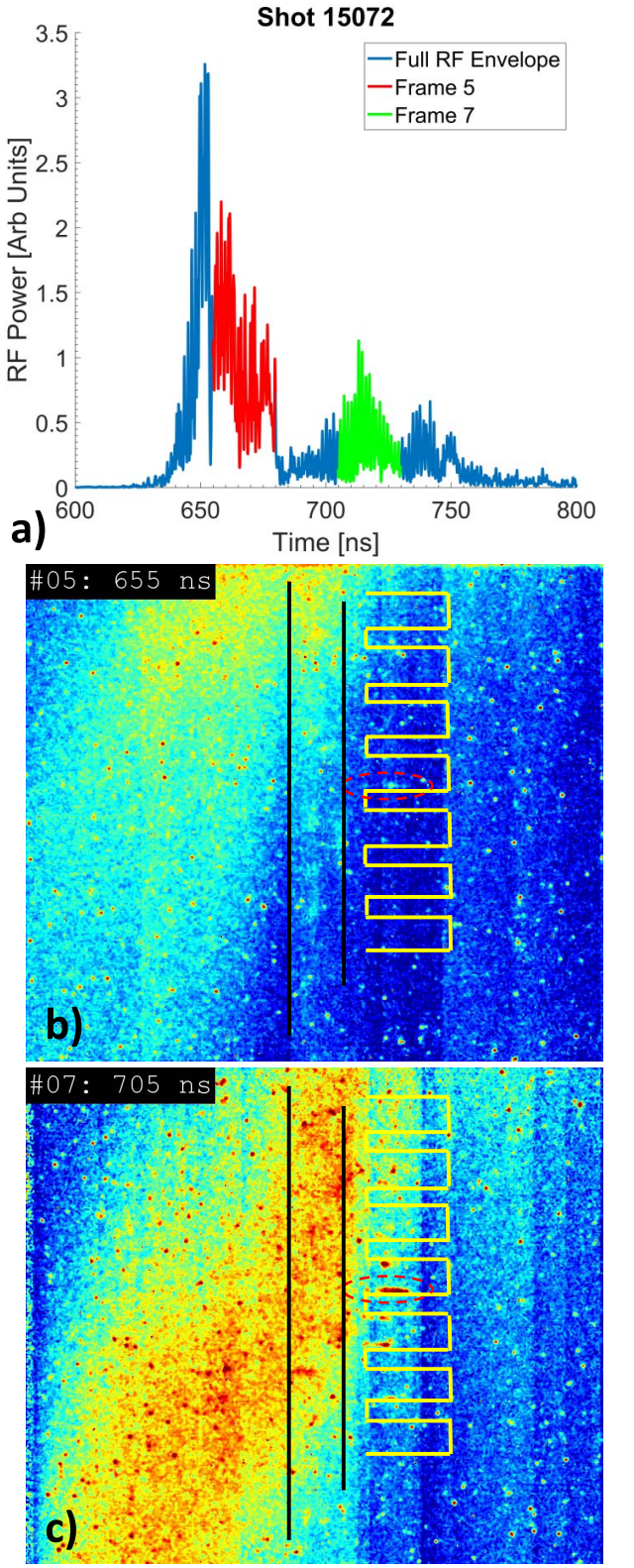


Fig. 6. (a) Frame timing and RF oscillations in shot 15072. (b) Intervane plasma formation is first observed in frame 5 correlating with a sharp decrease in microwave intensity. (c) Microwave oscillations restart and are extinguished during frame 7, as the anode plasma reaches peak intensity.

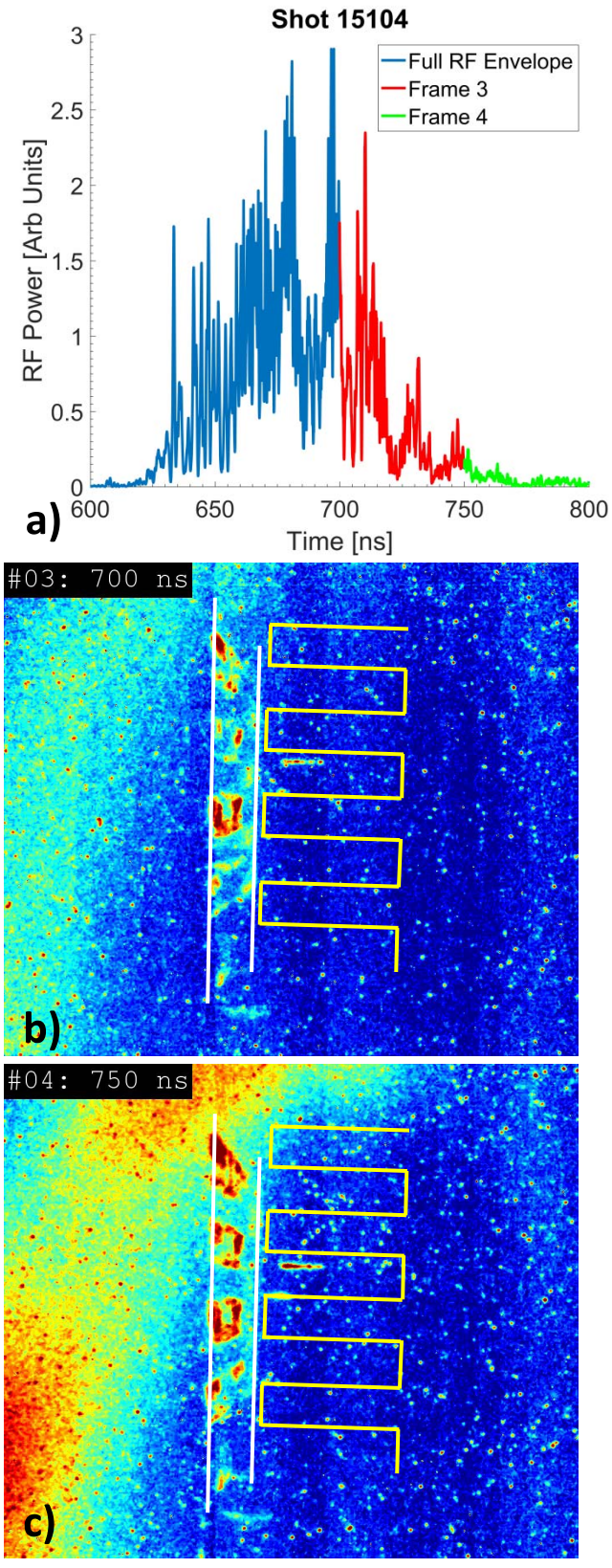


Fig. 7. (a) Frame timing and RF oscillations in shot 15104. (b) Intervane plasma formation again correlates with a sharp reduction in microwave power. (c) Significant cathode plasma is observed, concentrated in regions with Glyptal insulating enamel.

of a series often produced unusual results. Typically, the first few shots of a series were also the first few shots of the day,

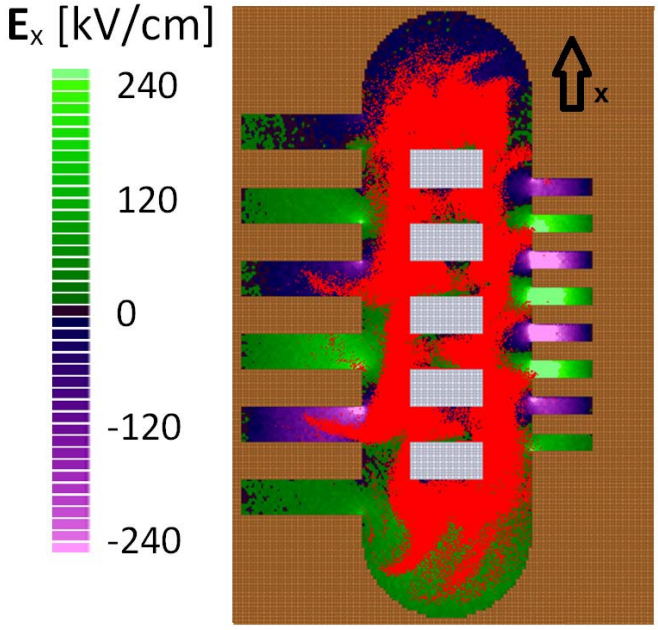


Fig. 8. Axial cross section of a MAGIC PIC simulation of $\pi$-mode MFRPM operation, indicating >200 kV/cm electric fields between anode vanes during typical magnetron operation with unoptimized extractor. Electron beam rotates counterclockwise.

and the pulsed power driver also experiences a short daily "break-in" period, so these anomalies should not be attributed strictly to anode/cathode conditioning. Qualitatively, plasma formation after the first few shots was consistent.

Anode plasma was consistently visible on the edges of the slow-wave structure, indicating electric field enhancement from the sharp vane edges was contributing to plasma formation. Future anodes should incorporate rounded vanes to minimize the electric field in these regions.

## V. Conclusion

Time-integrated visible light imaging of an RPM driven by a long-pulse Marx bank provided some insight into magnetron operation and plasma formation, but also captured substantial emissions well after the relevant microwave event. Time-resolved measurements, using an ultrafast framing camera, revealed the formation of intervane plasma which frequently correlated with a sharp reduction in microwave generation. While the plasma does not expand enough to fully fill the cavity and short the vanes, it may be sufficiently disruptive to change the resonant characteristics of the structure and shorten the microwave pulse. The change in operating mode observed during shot 15072 supports this assertion. Additionally, research on HPM compressors has shown a plasma column of only 1 mm diameter can be sufficient to disrupt microwave transmission [27].

Plasma generation at electrical contact points within the anode structure was also observed. While this is not generally an issue for hard-tube vacuum electronic devices with welds and brazing, it demonstrates the importance of making good electrical contact (or placing poor contacts far from the interaction region) in prototypes and university scale experiments.

Significant plasma formation on vane tips indicates the need for rounded anode structures to avoid field enhancement. Despite an axially narrow (∼2 cm) emission surface on the cathode, plasma initiation was routinely observed at the axial extremes of the 11-cm-long anode vanes.

Pulse shortening remains a substantial challenge for HPM devices. While the plasma formation mechanisms presented here may be dominant for this unique microwave source and pulsed power driver combination, they also highlight potential problems to be avoided in a variety of HPM source designs.

## REFERENCES


[1] R. M. Gilgenbach, Y. Y. Lau, D. M. French, B. W. Hoff, J. Luginsland, and M. Franzi, "Crossed field device," U.S. Patent 8 841 867 B2, Sep. 23, 2014. [Online]. Available: https://www.google.com/patents/US8841867

[2] R. M. Gilgenbach, Y.-Y. Lau, D. M. French, B. W. Hoff, M. Franzi, and J. Luginsland, "Recirculating planar magnetrons for high-power high-frequency radiation generation," *IEEE Trans. Plasma Sci.*, vol. 39, no. 4, pp. 980–987, Apr. 2011.

[3] D. Price, J. S. Levine, and J. N. Benford, "Diode plasma effects on the microwave pulse length from relativistic magnetrons," *IEEE Trans. Plasma Sci.*, vol. 26, no. 3, pp. 348–353, Jun. 1998.

[4] M. D. Haworth, J. W. Luginsland, and R. W. Lemke, "Evidence of a new pulse-shortening mechanism in a load-limited MILO," *IEEE Trans. Plasma Sci.*, vol. 28, no. 3, pp. 511–516, Jun. 2000.

[5] A. Neuber, J. Dickens, D. Hemmert, H. Krompholz, L. L. Hatfield, and M. Kristiansen, "Window breakdown caused by high-power microwaves," *IEEE Trans. Plasma Sci.*, vol. 26, no. 3, pp. 296–303, Jun. 1998.

[6] M. D. Haworth *et al.*, "Significant pulse-lengthening in a multigigawatt magnetically insulated transmission line oscillator," *IEEE Trans. Plasma Sci.*, vol. 26, no. 3, pp. 312–319, Jun. 1998.

[7] J. G. Leopold, A. S. Shlapakovski, A. F. Sayapin, and Y. E. Krasik, "Pulse-shortening in a relativistic magnetron: The role of anode block axial endcaps," *IEEE Trans. Plasma Sci.*, vol. 44, no. 8, pp. 1375–1385, Aug. 2016. [Online]. Available: https://doi.org/10.1109/TPS.2016.2580613

[8] M. C. Jones, "Cathode priming of a relativistic magnetron using multi-emission zones on projection ablation lithography cathodes," Ph.D. dissertation, Dept. Nuc. Eng., Univ. Michigan, Ann Arbor, MI, USA, 2005. [Online]. Available: http://hdl.handle.net/2027.42/125111

[9] F. J. Agee, "Evolution of pulse shortening research in narrow band, high power microwave sources," *IEEE Trans. Plasma Sci.*, vol. 26, no. 3, pp. 235–245, Jun. 1998.

[10] M. A. Franzi *et al.*, "Microwave power and phase measurements on a recirculating planar magnetron," *IEEE Trans. Plasma Sci.*, vol. 43, no. 5, pp. 1675–1682, May 2015.

[11] M. A. Franzi *et al.*, "Recirculating-planar-magnetron simulations and experiment," *IEEE Trans. Plasma Sci.*, vol. 41, no. 4, pp. 639–645, Apr. 2013. [Online]. Available: http://dx.doi.org/10.1109/TPS.2013.2242493

[12] T. A. Treado, R. S. Smith, C. S. Shaughnessy, and G. E. Thomas, "Temporal study of long-pulse relativistic magnetron operation," *IEEE Trans. Plasma Sci.*, vol. 18, no. 3, pp. 594–602, Jun. 1990.

[13] I. Z. Gleizer, A. N. Didenko, A. S. Sulakshin, G. P. Fomenko, and V. I. Tsvetkov, "Limitation on the duration of the microwave emission in a high-current magnetron," *Sov. Phys.-Tech. Phys. Lett.*, vol. 6, p. 19, Jan. 1980.

[14] M. E. Cuneo, "The effect of electrode contamination, cleaning and conditioning on high-energy pulsed-power device performance," *IEEE Trans. Dielectr. Electr. Insul.*, vol. 6, no. 4, pp. 469–485, Aug. 1999.

[15] G. B. Greening, M. Franzi, R. Gilgenbach, Y. Y. Lau, and N. Jordan, "Multi-frequency recirculating planar magnetrons," Ph.D. dissertation, Dept. Nucl. Eng., Univ. Michigan, Ann Arbor, MI, USA, 2017. [Online]. Available: https://deepblue.lib.umich.edu/handle/2027.42/138623

[16] M. R. Lopez *et al.*, "Relativistic magnetron driven by a microsecond E-beam accelerator with a ceramic insulator," *IEEE Trans. Plasma Sci.*, vol. 32, no. 3, pp. 1171–1180, Jun. 2004.

[17] G. B. Greening, N. M. Jordan, S. C. Exelby, D. H. Simon, Y. Y. Lau, and R. M. Gilgenbach, "Multi-frequency recirculating planar magnetrons," *Appl. Phys. Lett.*, vol. 109, no. 7, p. 74101, Aug. 2016. [Online]. Available: http://dx.doi.org/10.1063/1.4961070

[18] M. Franzi, R. Gilgenbach, Y. Y. Lau, B. Hoff, G. Greening, and P. Zhang, "Passive mode control in the recirculating planar magnetron," *Phys. Plasmas*, vol. 20, no. 3, p. 033108, 2013.

[19] Y. M. Saveliev, S. N. Spark, B. A. Kerr, M. I. Harbour, S. C. Douglas, and W. Sibbett, "Effect of cathode end caps and a cathode emissive surface on relativistic magnetron operation," *IEEE Trans. Plasma Sci.*, vol. 28, no. 3, pp. 478–484, Jun. 2000.

[20] C. Leach, S. Prasad, M. I. Fuks, and E. Schamiloglu, "Suppression of leakage current in a relativistic magnetron using a novel design cathode endcap," *IEEE Trans. Plasma Sci.*, vol. 40, no. 8, pp. 2089–2093, Aug. 2012.

[21] C. W. Peters *et al.*, "Application of time-frequency analysis to high-power microwave devices," *Proc. SPIE*, vol. 4116, pp. 1–8, Nov. 2000, [Online]. Available: http://dx.doi.org/10.1117/12.406494

[22] *MAGIC Tool Suite, Version 3.2.5.8*, Alliant Techsystems, Falls Church, VA, USA, 2014. [Online]. Availablel: https://www.orbitalatk.com/MAGIC/

[23] O. T. Loza, A. G. Shkvarunets, and P. S. Strelkov, "Experimental plasma relativistic microwave electronics," *IEEE Trans. Plasma Sci.*, vol. 26, no. 3, pp. 615–627, Jun. 1998.

[24] D. Price and J. Benford, "General scaling of pulse shortening in explosive-emission-driven microwave sources," *IEEE Trans. Plasma Sci.*, vol. 26, no. 3, pp. 256–262, Jun. 1998.

[25] Y. Hadas, A. Sayapin, Y. E. Krasik, V. Bernshtam, and I. Schnitzer, "Plasma dynamics during relativistic *S*-band magnetron operation," *J. Appl. Phys.*, vol. 104, no. 6, p. 064125, Sep. 2008. [Online]. Available: https://doi.org/10.1063/1.2986520

[26] T. Queller, J. Z. Gleizer, and Y. E. Krasik, "Secondary-electrons-induced cathode plasma in a relativistic magnetron," *Appl. Phys. Lett.*, vol. 101, no. 21, p. 214101, Nov. 2012. [Online]. Available: https://doi.org/10.1063/1.4767953

[27] L. Beilin, A. Shlapakovski, M. Donskoy, T. Queller, and Y. E. Krasik, "Plasma density temporal evolution in a high-power microwave pulse compressor switch," *EPL*, vol. 109, no. 2, p. 25001, 2015. [Online]. Available: https://doi.org/10.1209/0295-5075/109/25001

[28] N. M. Jordan *et al.*, "Pulse shortening in recirculating planar magnetrons," in *Proc. Int. Vac. Electron. Conf. (IVEC)*, London, U.K., Apr. 2017.


Authors' photographs and biographies not available at the time of publication.